

# Efficient Coupling of Electrostatic Optical Fiber Switch

Cheng-Tang Pan\*, Sheng-Chih Shen<sup>1</sup> and Hsiharng Yang<sup>2</sup>

Department of Mechanical and Electro-Mechanical Engineering,  
and Center for Nanoscience & Nanotechnology, National Sun Yat-Sen University,  
Kaoshiung 804, Taiwan

<sup>1</sup>Mechanical Industry Research Laboratories, Industrial Technology Research Institute,  
Hsinchu 310, Taiwan

<sup>2</sup>Institute of Precision Engineering, National Chung Hsing University, Taichung, Taiwan 402

(Received June 23, 2003; accepted November 25, 2003)

**Key words:** out-of-plane, micro-ball lens, optical switch, diaphragm, electrostatic, coupling

The study presents a novel concept of a coupling platform integrated with an out-of-plane optical switch and micro-ball lens array. The micro-ball lens array is batch-fabricated with the micro electro mechanical system (MEMS) technique and batch-assembled onto the platform. The out-of-plane optical switch consists of a self-latching vertical mirror on a suspension diaphragm. It can reduce the large motion space required for in-plane optical switches. The optical platform design enables control of the distance between the fiber, micro-ball lens and out-of-plane optical switch and increases their coupling efficiency. An electrostatic driving voltage is used to actuate the optical switch. Not only does this fabrication process provide an accurate coupling distance, it also reduces the micro-assembly cost.

## 1. Introduction

An optical switch is an important component for a variety of applications in optics communication, especially in the field of optical fiber networks because it requires large quantities of optical components.<sup>(1-2)</sup> Therefore, low manufacturing costs and high-speed optical switches are necessary for an efficient light transmission system and network safety. Microactuator structures are based on MEMS technology and have been used for

---

\*Corresponding author, e-mail address: panct@mail.nsysu.edu.tw

moving the micromirror structures in torsion beams,<sup>(3-4)</sup> rotary micromotors,<sup>(5)</sup> comb drives,<sup>(6-7)</sup> bistable mechanics,<sup>(8)</sup> and U-shaped cantilevers.<sup>(9)</sup> Previous work has already discussed a lot about the fabricating the V-groove using anisotropic etching, improving the smoothness of the mirror surfaces and optical switch performance. However, it has not discussed how to improve the coupling efficiency from fiber to optical element. The conventional method to fabricate an optical switch is to form a high-refractive-index ball lens at the fiber's terminal to enhance fiber optical coupling efficiency. Fibers are first arc discharged and cut. Then, a ball lens is formed following the process of immersing tapered fiber into molten glass.<sup>(10,11)</sup> Another conventional method involves assembling a micro-ball lens to improve coupling efficiency. However, these procedures are time consuming. Furthermore, there exist numerous papers on how to batch fabricate a micro-lens array<sup>(12-14)</sup> applying on optical communications, but few discuss the micro-ball lens.

In this paper, a novel design and fabrication of silicon-based optical coupling platform in free space has been proposed. At the platform, a micro-ball lens is designed between the optical fiber and out-of-plane optical switch to minimize coupling loss. This out-of-plane optical switch consists of a self-latching vertical mirror on a suspension diaphragm. This design reduces the large motion space required in in-plane optical switches. The micro-mirror is located on a membrane suspended by four cantilever beams and driven by an electrostatic force. This design for the platform not only simplifies the process, but also requires less time for device fabrication. In the following sections, the mechanism and fabrication of the out-of-plane optical switch will be discussed in details.

## 2. Design

A three dimensional schematic illustration of an out-of-plane optical switch is shown in Fig. 1. This coupling platform includes a micro-ball lens, an out-of-plane optical switch, and a self-parking framework. The micro-ball lens was designed between the optical fiber and out-of-plane optical switch to minimize coupling loss. This out-of-plane optical switch consists of a vertical mirror which can self-park on the flat-topped mesa. The flat-topped mesa is located at the intersection of two v-grooves. It is designed to park the vertical mirror, to reduce the mechanical bounce of the vertical mirror and to increase the actuator dynamic response during the motion. This design reduces the large motion space required in in-plane optical switches. The vertical mirror with a 45 degree inclination to the v-groove is located on a suspension diaphragm supported by four cantilever beams and driven by electrostatic force. A vertical mirror was arranged in the coupling platform to compose an optical crossbar switch. When a bias voltage is applied, the vertical mirror on the PI diaphragm will be attracted upward and will not interrupt the incident light. The optical switch is in an ON-state position. Its cross-section view and 3-D illustration are shown in Fig. 1(a). The incident light can propagate through two micro-ball lenses to the opposite fiber. Otherwise, when the voltage is off, the mechanical restoration force of the suspension beams pulls the vertical mirror downward elastically from the ON-state position. The vertical mirror will touch the flat-topped mesa as a stopper at the intersection of v-grooves, and the diaphragm will hold horizontally as shown in Fig. 1(b). Then the optical switch is in the OFF-state position. Hence it will reflect the incident light and

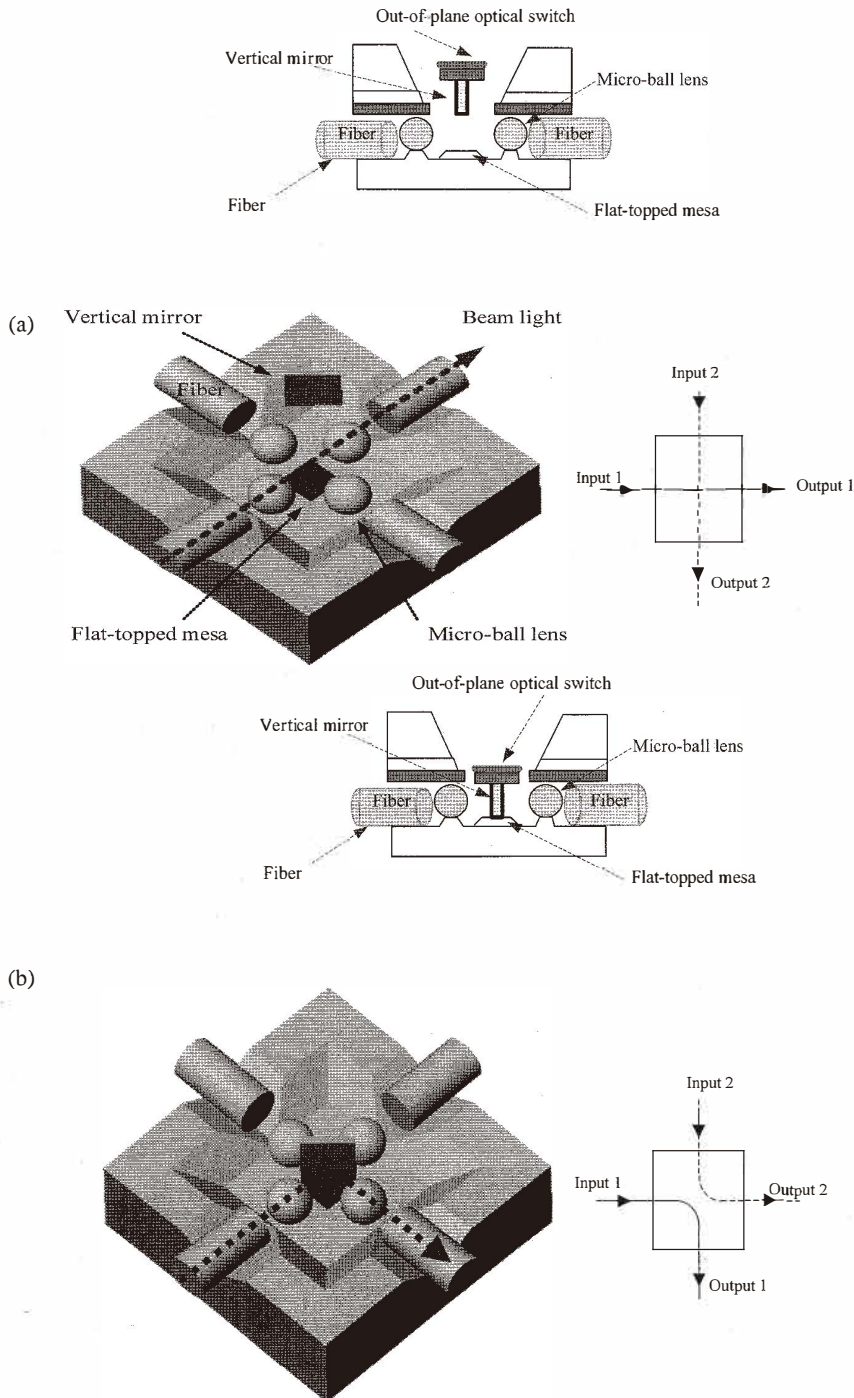


Fig. 1. Schematic 3-D cross-section view of the novel coupling platform. (a) ON state (b) OFF state

redirect it to the orthogonal fiber. The optical coupling platform can improve optical coupling in free space, enhance frequency and solve some problems, such as the micro-assemblage micro-ball lens array and long distance optical coupling. With this design of platform, it will not only simplify the process, but also take less time to finish the device. In the following sections, the mechanism and fabrication of out-of-plane optical switches will be discussed in detail.

### 2.1 Principle of out-of-plane optical switch

The out-of-plane optical switch consists of a self-latching vertical mirror on the top substrate. The vertical mirror is supported by a suspension polyimide (PI) diaphragm with four cantilever beams. In the optical switch, the PI-based flexible actuator membrane is batch-fabricated and coated with a thin film of Ag metal using sputtering as an electrode. Since PI has excellent mechanical properties such as a low Young's modulus (less than 3 Gpa), high glass transition temperature ( $T_g$ ) and good flexibility, it can provide higher displacement compared with other micro-actuators. Excimer laser ablation is used to pattern the PI membrane.

The vertical mirror was driven by electrostatic operation. The light emitted from the input fiber can be precisely transmitted through the micro-ball lenses to the opposite fiber when the vertical mirror is moved up. When the voltage is off, the mechanical restoration force of the suspension arms pulls the vertical mirror down and latches it to the mesa. The light beam through the micro-ball lenses then impinges on the vertical mirror and precisely redirects it to the orthogonal fiber. The PI layer coated onto the mesa reduces the mechanical bounce in the ON/OFF state and also restrains the vertical mirror. A self-latching vertical mirror is thus produced.

The suspension diaphragm of the optical switch is designed with equal lengths of diaphragm beams and a straight uniform cross section. This diaphragm is made of a homogeneous isotropic material that obeys Hook's Law. The maximum displacement ( $\delta$ ) of the suspension diaphragm can be expressed as<sup>(15)</sup>

$$\delta = \frac{F \cdot l^3}{96EI} \quad (1)$$

where the parameter  $F$  is the electrostatic force;  $E$  is the elastic modulus of the diaphragm beam;  $I = bt^3/12$  is the moment of inertia of the cantilever beam and  $l$  is the beam length.

The dimension of the optical switch is preliminarily designed by ANSYS software considering the resonant frequency and displacement. The optical switch dimensions are  $150 \mu\text{m}$  (width)  $\times 75 \mu\text{m}$  (height)  $\times 20 \mu\text{m}$  (thickness) for the vertical mirror,  $800 \mu\text{m}$  (width)  $\times 800 \mu\text{m}$  (height)  $\times 10 \mu\text{m}$  (thickness) for the suspension diaphragm, and  $1000 \mu\text{m}$  (length)  $\times 50 \mu\text{m}$  (width)  $\times 10 \mu\text{m}$  (thickness) for the support beams.

### 2.2 Principle of micro-ball lens

In a dual-layer system, as shown in Fig. 2, the photoresist (labeled as M2) and polymer (labeled as M1) are spin-coated on the substrate followed by exposure and development.<sup>(16)</sup>

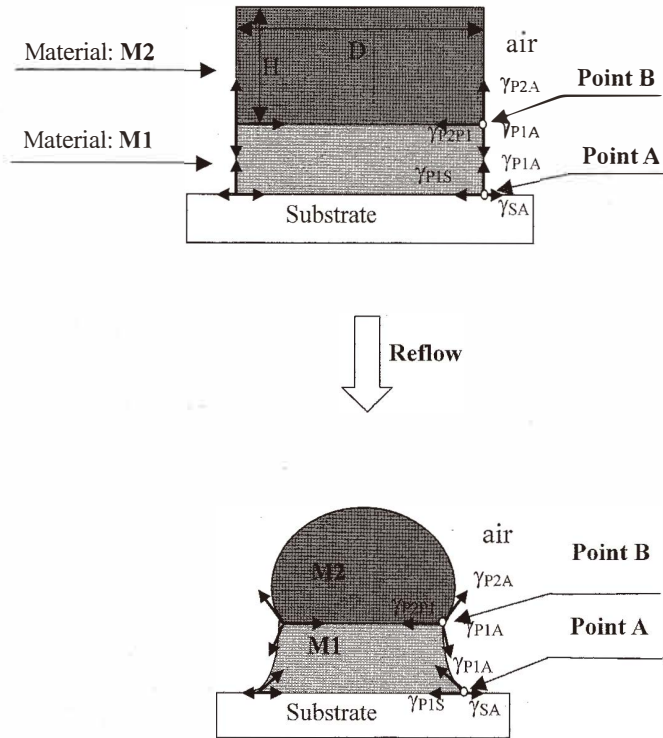


Fig. 2. Theoretical surface tensions in dual-layer system for micro-ball lens fabrication.

When the system is heated above  $T_g$  the temperature of the photoresist (M2) in an oven, it begins to show liquid behavior and to reduce the surface energy. The applied reflow temperature is lower than the  $T_g$  of polymer (M1). As the temperature increases, points A and B are not at equilibrium. The induced force tends to pull point B toward the center of the column until all surface tension at points A and B is at equilibrium. Theoretically, this column of two-layer polymeric material tends to decrease the surface energy when the applied reflow temperature increases. After the reflow process, the final profile of the column becomes spherical due to its low surface energy.

Young's Model describes the surface tension of a liquid droplet on a solid surface as:<sup>(17)</sup>

$$T_{SA} = T_{LS} + T_{AL} \cos \theta \quad (2)$$

where  $\theta$  is the equilibrium contact angle,  $T_{AL}$  is the surface tension of the liquid,  $T_{SA}$  is the surface energy of the solid, and  $T_{LS}$  is the solid-liquid interface energy.

### 3. Fabrication

#### 3.1 Out-of-plane optical switch

The top plate process, the flow chart is shown in Fig. 3. Firstly, a  $1.5\ \mu\text{m}$  thick thermal  $\text{SiO}_2$  film was grown using wet oxidization at  $1100^\circ\text{C}$  on a double side polished (100) silicon wafer as shown in Fig. 3(a). The bulk etching area was patterned on the backside by mask number 1. Wet oxidization is regarded as the etching mask. Then the PI layer was spin-coated on the upper side of the silicon wafer. After fully curing the PI at  $350^\circ\text{C}$ , the PI film was  $10\ \mu\text{m}$  thick. Then, vertical mirror was patterned on the PI layer using a photoresist SU-8, followed by Au sputtering to enhance the surface reflectivity as shown in Fig. 3(e). Under the protection of a Teflon chuck, back etching was done using bulk

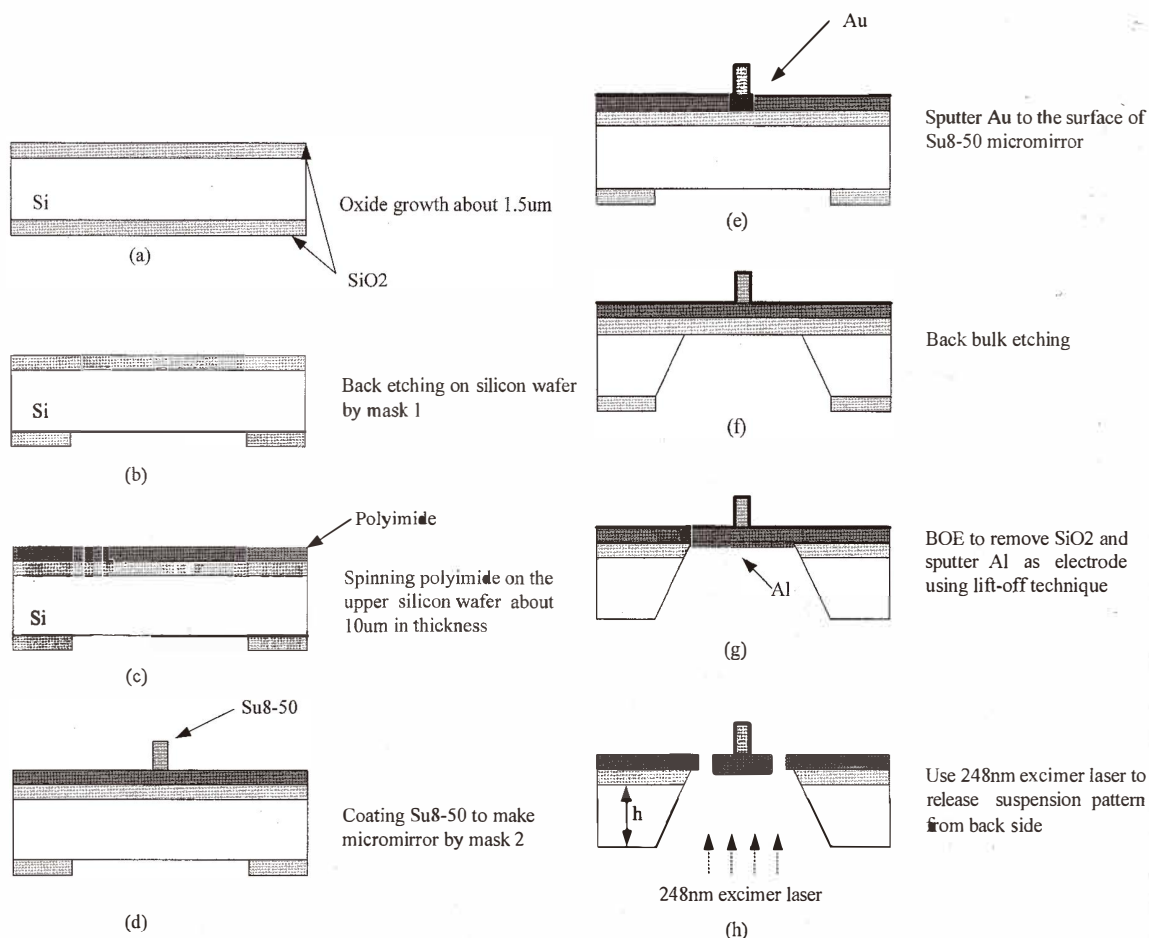


Fig. 3. Schematic fabrication flow chart of top plate.

micromachining techniques. The whole wafer was immersed into 30 wt% aqueous KOH solution at 70°C until the dioxide etch stop layer on the upper side appears as shown in Fig. 3(f). Then the dioxide layers were removed with BOE solution, followed by sputtering Al as an electrode by lift-off technique.

Finally, an Exitech 8000 excimer laser workstation was used to pattern the PI patterns. The laser was from Lambda Physik COMPex-110 industrial model with 248 nm wavelength, 400 mJ pulse energy, 25 ns pulse duration time, and 100 Hz peak pulse repetition rate. The geometry of suspension microbeams on the diaphragm was ablated and defined precisely using excimer laser micromachining. In this experiment, it is worth noticing that this process demonstrated that a PI diaphragm could be patterned by excimer laser ablation after it was released from anisotropic wet etching. Besides, the diaphragm has to be ablated from the backside of the wafer to avoid unexpected vibrations caused by plasma during ablation as shown in Fig. 3(h). These vibrations could change the focus plane of the workpiece and affect the pattern geometry.

The prototype of the out-of-plane optical switch is illustrated in Fig. 4. The sandwich substrates with fibers were glued using an SU-8 resist. The top substrate was made of a double-polished (100)-oriented silicon wafer. In this fabrication process, the optical switch was patterned after it was released from the substrate. Moreover, thick photoresist lithography, bulk micromachining, and excimer laser ablation improved the flexibility of process.

### 3.2 Micro-ball lens

AZ4620 and SP341 were selected as the photoresist and polymer, respectively. AZ4620 was purchased from Clariant Company in Japan. Its ingredients mainly include propylene glycol monomethyl ether acetate, a naphthoquinone diazide derivative as well as some additives, and its  $T_g$  is between 175°C and 180°C. As for SP341, its substance is a PI-based material with  $T_g$  of about 300°C, purchased from the Toray Company. The polymer SP341 was smoothly spin-coated on the hot-dried wafer followed by AZ4620 spread on.

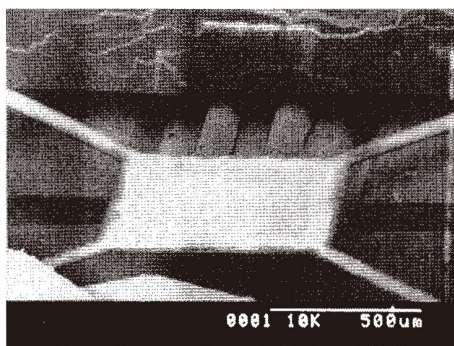


Fig. 4. Out-of-plane optical switch. SEM view of the 2 × 2 out-of-plate micro-optical switch.

The exposure and development were carried out to build a cylinder of dual layers on the wafer. The wafer was then placed in an oven for reflow to produce a micro-ball lens array.

The rotational speed of spin-coating determined the layer thickness of the photoresist. The higher the rotational speed, the lower is the thickness. The speeds of 600, 800, 1000 and 1200 rpm produce thicknesses of 33, 26, 18 and 15  $\mu\text{m}$ , respectively. The exposure dose is 520  $\text{mJ}/\text{cm}^2$  for 40 s. The oven temperature was set at 190°C, 220°C and 250°C.

The microscope, SEM and interferometer were used to measure the profile of the micro-ball lens. The experimental results of the micro ball lens are shown in Fig. 5.

#### 4. Results and Discussion

The coupling platform has successfully combined a  $2 \times 2$  optical switch with micro-ball lens. The micro-ball lens was characterized and tested. The measurement is illustrated in Fig. 6. Visible 653 nm laser diode was collimated into the micro-ball lens 40  $\mu\text{m}$  in diameter. Visible light passed through and focused on the micro-ball lens as shown in Fig. 7(a). The single-mode laser beam was focused and collimated onto the micro-ball lens 40  $\mu\text{m}$  in diameter. The coupling efficiency was measured by light intensity with variation of the distance between the micro-ball lens and the fiber. Each coupling position from the fiber to the micro-ball lens was measured with a fixed distance between the laser diode and the micro-ball lens. The focal length of the micro-ball lens depends on the refractive index of the lens, the radius of curvature, and the thickness along the optical axis. Figure 7(b)

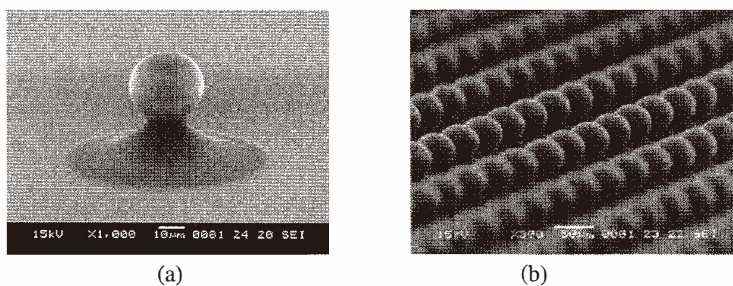


Fig. 5. Formation of micro-ball lens. (a) Single ball (b) In arrays

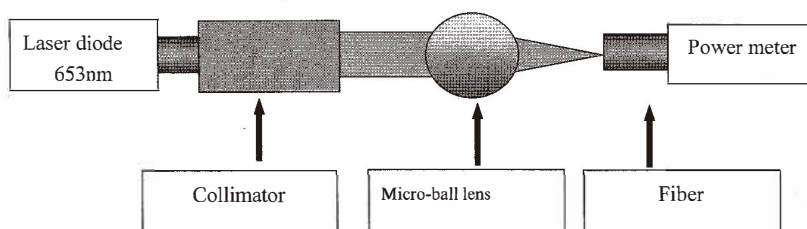


Fig. 6. Experimental setup of coupling measurement.

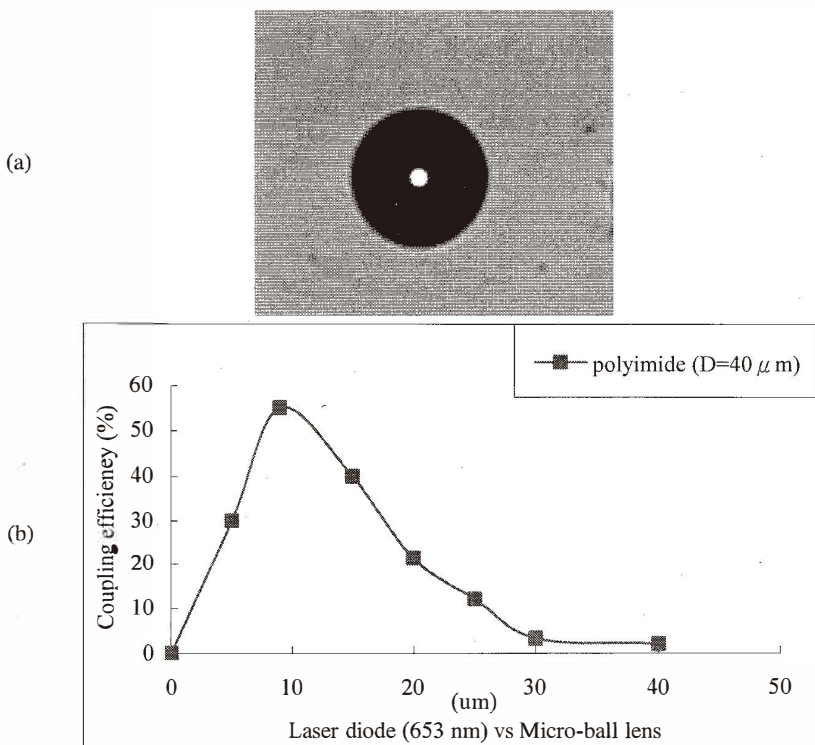


Fig. 7. Measurement of coupling efficiency with micro-ball lens arrangement. (a) Photograph of the visible light focused by micro-ball lens. (b) Coupling efficiency of micro-ball lens.

shows that the light beam was focused by the micro-ball lens. It also reveals that the experimental measurement of coupling efficiency is a function of distance from the fiber and micro-ball lens. In this optical coupling platform, the optimal coupling distance is about  $9 \mu\text{m}$  and the insertion loss is about  $-1.1 \text{ dB}$ . Therefore, using this fabrication process not only provides accurate coupling distance between fibers and micro ball lens, but also reduces micro-assembly cost. This study shows that an inexpensive and batch micro-assembly micro-ball lens array process can be used to replace the traditional methods, such as that using an aspherical lens or expensive GRIN, without sacrificing performance.

The out-of-plane optical switch consists of a suspension diaphragm and a vertical mirror. The vertical mirror requires an extraordinarily smooth surface for high reflectivity. The mirror surface roughness was improved using a thick SU-8 photoresist applied using photolithography and an Au sputter deposition  $170 \text{ nm}$  thick. The vertical mirror sidewall was measured using AFM (atomic force microscopy). The result is shown in Fig. 8. The vertical mirror has a surface roughness below  $20 \text{ nm rms}$ . The laser beam of a single-mode

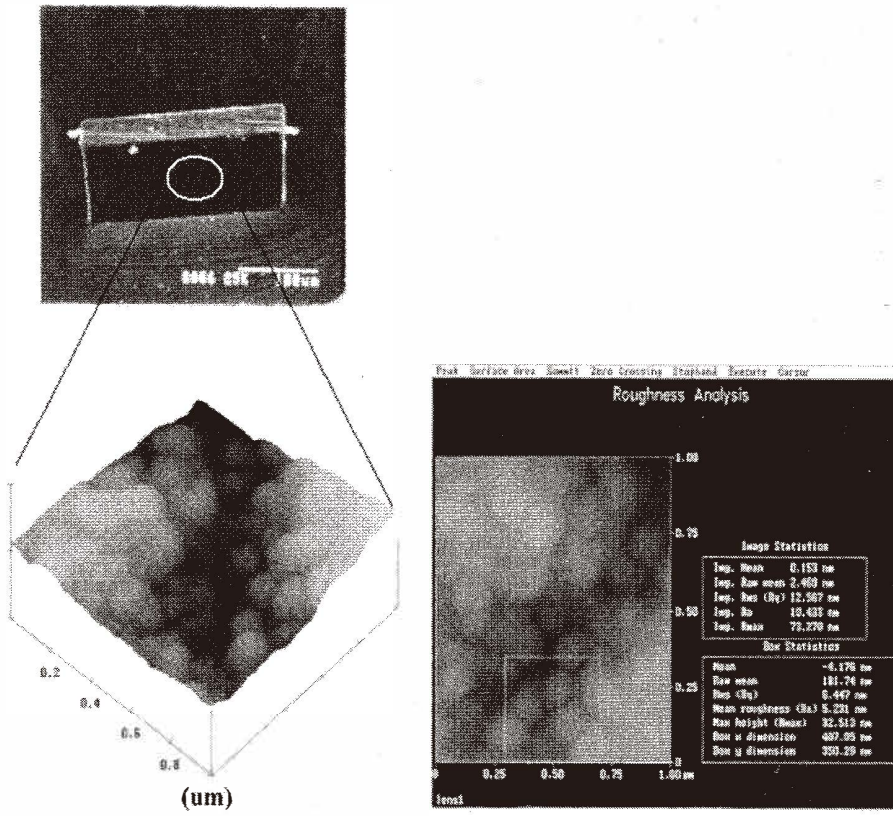


Fig. 8. Surface roughness of the vertical mirror measured using AFM.

fiber laser was focused and collimated onto the vertical mirror  $75 \mu\text{m}$  in height. The intensity of reflected light was redirected and measured using a power-meter.

The out-of-plane optical switch is electrostatically driven. The relationship between the electrostatic force and suspension diaphragm displacement is shown in Fig. 9. An actuator voltage of 100 V is required for a  $2 \times 2$  switch. The displacement of the suspension diaphragm is  $48 \mu\text{m}$  at 100 V. The optical switch dynamic response is shown in Fig. 10. The driving voltage is shown on the top waveform and the dynamic signal is shown at the bottom waveform. The figure reveals that the optical switch can operate 4 cycles from 24.3 to 24.302 s. This means that 2 kHz can be achieved.

The PI diaphragm was continuously operated at a room temperature of  $22^\circ\text{C}$  for 30 min at 2 kHz. The overall size of the switch was less than  $1 \text{ mm}^3$ . A wavelength of 653 nm was used to measure the insertion loss. A thermal expanded core (TEC) fiber with a fiber core  $20 \mu\text{m}$  in diameter was used. The TEC and single fibers could expand the coupling distance to 1 mm inducing an insertion loss of  $-2.5 \text{ dB}$ . When the moving mirror is up, the

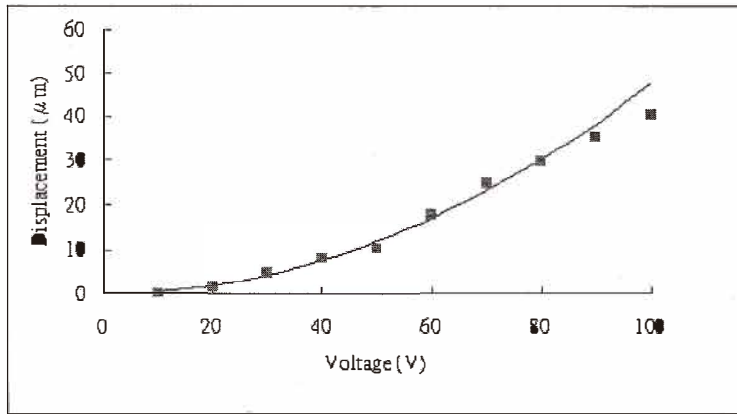


Fig. 9. Relationship between the electrostatic force and suspension diaphragm displacement.

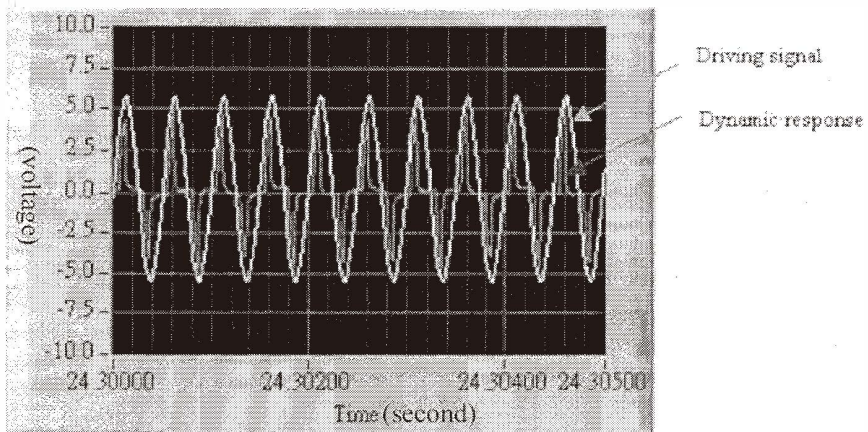


Fig. 10. Measured input signal waveform and optical dynamic switch response.

light emitted from the input can be precisely transmitted to the opposite fiber and the insertion loss is  $-2.1$  an insertion loss of  $-3.5$  dB. During the optical measurement, the fiber assemblers are actively aligned, because a  $0.5^\circ$  misalignment induces a loss of  $-2.5$  dB.

## 5. Conclusion

An out-of-plane optical switch array was presented to solve several existing problems. The vertical mirror structure can be fabricated using a thick photoresist SU-8 through UV

lithography and sputtered with gold film. The roughness of the mirror surface was less than 20 nm rms. The optical switch has a maximum displacement of 48  $\mu\text{m}$  and the switching time is shorter than 0.4 ms with a driving voltage of 100 VDC. The experimental measurement of optimum coupling distance between the fiber and micro-ball lens is about 9  $\mu\text{m}$ , and the insertion loss is about -3 dB. We successfully demonstrated that the coupling platform consists of the out-of-plane optical switch, and micro-ball lens. The fabrication process not only provides accurate coupling distance, but also reduces micro-assembly cost.

### Acknowledgement

The author would like to thank Dr. Tung-Chuan Wu and Dr. Min-Chan Chou at MIRL of ITRI in Taiwan for their guidance, and National Science Council (NSC) for their financial supports to the project (granted number: NSC92-2622-E110-009-CC3 and NSC92-2212-E110-029).

### References

- 1 H. Fujita: Microactuators and Micromachine, Proceedings of the IEEE (1998) p. 1721.
- 2 W. S. N. Trimmer: Sensors and Actuators A **70** (1989) 267.
- 3 H. Toshiyoshi and H. Fujita: IEEE J. Microelectromech. Syst. **5** (1996) 231.
- 4 H. Toshiyoshi, D. Miyauchi and H. Fujita: IEEE J. Selected Topics in Quantum Electronics **5** (1999) 10.
- 5 A. A. Yasseen, J. N. Mitchell, J. F. Klemic and D. A. Smith: IEEE J. Microelectromech. **5** (1999) 26.
- 6 C. Marxer, C. Thio, M. A. Gretillat and N. F. Rooij: IEEE J. Microelectromech. Syst. **6** (1997) 277.
- 7 W. H. Juan and S. W. Pang: IEEE J. Microelectromech. Syst. **7** (1998) 207.
- 8 M. Hoffmann, P. Kopka and E. Voges: IEEE J. Microelectromech. Syst. **5**, (1997) 211.
- 9 Peter Kopka, Martin Hoffmann, Edgar Voges: J. Micromech. Microeng. **10** (2000) 260.
- 10 Vera Russo, Giancarlo C. Righini, Stefano Sottini and Silvana Trigari: Applied Optics **23** (1984) 3277.
- 11 G. D. Khoe, J. Poulissen and H. M. de Vrieze: Electronics Letters **19** (1983) 205.
- 12 D. Daly, R. F. Stevens, M. C. Hutley and N. Davies, Meas. Sci. Technol. **1** (1990) 759.
- 13 Zoran D. Popovic, Robert A. Sprague and G. A. Neville Connell: Applied Optics **27** (1988) 1281.
- 14 M. C. Hutley, R. F. Stevens and D. Daly: The Manufacture of Microlens Arrays and Fan-Out Gratings in Photoresist, Optical Connection and Switching Networks for Communication and Computing (1990) p. 11/1.
- 15 E.P. Popov, Nagarajan, Sambamurthy Lu and Aung An: Mechanics of materials (Prentice-Hall, Englewood Cliffs, N.J, 1976).
- 16 Y.-S. Lin, C. T. Pan, K.-L. Lin, S.-C. Chen, J.-J. Yang, and J.-P. Yang: Polyimide as the Pedestal of Batch Fabricated Micro-Ball Lens and Micro-Mushroom Array (MEMS 2001 14<sup>th</sup>, 2001) p. 337.
- 17 C.U. Lin: New method of measurement of surface tension and contact angle, technical report NSC85-2214-E011-018 (1997).